Self-Assembly of Functionalized [2]Catenanes Bearing a Reactive Functional Group on either One or Both Macrocyclic Components—From Monomeric [2]Catenanes to Polycatenanes†

Stephan Menzer, Andrew J. P. White, and David J. Williams

Department of Chemistry, Imperial College, South Kensington, London SW7 2AY, U.K.

Martin Bělohradský, Christoph Hamers, Françisco M. Raymo, Andrew N. Shipway, and J. Fraser Stoddart*

School of Chemistry, University of Birmingham, Edgbaston, Birmingham B15 2TT, U.K.

Received May 16, 1997; Revised Manuscript Received October 20, 1997

ABSTRACT: A series of mono- and difunctionalized [2]catenanes, incorporating a bipyridinium-based cyclophane component interlocked with a dioxyarene-based macrocyclic polyether, have been self-assembled. The methodology relies upon the complementarity between the π-electron-deficient and the π-electron-rich macrocyclic components. Hydrogen-bonding interactions between the acidic hydrogen atoms on the bipyridinium units and the polyether oxygen atoms, as well as $\pi-\pi$ stacking and edge-to-face T-type interactions between the complementary aromatic units, are responsible for these self-assembly processes. These [2]catenanes have been designed in order to locate one reactive functional group—either a hydroxyl group or a carboxylic acid function—onto one or both macrocyclic components. In principle, polymerization or copolymerization of these monomeric [2]catenanes can be realized by condensations at the reactive functional groups to generate main-chain, side-chain, and dendritic polycatenanes. Indeed, the versatility of this design logic has been demonstrated by some preliminary experiments. A main-chain oligo[2]catenane incorporating 17 repeating units connected by urethane linkages was synthesized by the condensation of a monomeric difunctionalized [2]catenane bearing one hydroxymethyl group on each of its two macrocyclic components with a diisocyanate derivative. The geometries adopted in the solid state by some of the monomeric [2]catenanes were examined by single-crystal X-ray analyses. Interestingly, in the case of a monofunctionalized [2]catenane bearing one carboxylic acid group on its π-electron-rich macrocyclic component, pseudobis[2]catenanes are observed in the solid state as a result of the formation of hydrogen-bonded dimers between the carboxylic acid groups of adjacent molecules.

Introduction

The interest of many investigators is now being focused on the synthesis of a new class of polymeric materials composed of macrocyclic components linked by mechanical bonds—namely, polycatenanes.[1] The main-chain polycatenane (a), schematically represented in Figure 1, is the equivalent of a chain at the molecular level. However, its synthesis is not easily achievable and the highest homolog of this class of compounds self-assembled so far is the so-called Olympiadane[2]—namely, a [5]catenane incorporating five interlocked rings in a linear array. The main-chain polycatenanes (b) and (c) feature the alternation of covalent and mechanical bonds—the latter embellished with noncovalent bonding interactions—along their main axes. These compounds can be synthesized, in principle, by polymerization or copolymerization, respectively, of [2]catenane[3] monomers possessing one reactive functional group on each of the two macrocyclic components. Similarly, monofunctionalized [2]catenane monomers can be grafted on to a polymeric backbone or attached to a highly branched core to afford side-chain (d) or dendritic polycatenanes.

Recently, we have developed[4] a synthetic methodology to self-assemble[5] [*n*]catenanes incorporating π-electron-rich dioxyarene-based macrocyclic polyethers interlocked with π-electron-deficient bipyridinium-based cyclophanes. Noncovalent bonding interactions between the complementary components—namely, $\pi-\pi$ stacking[6,7] and edge-to-face[7,8] T-type interactions between the aromatic units as well as hydrogen bonding[9,10] between the polyether oxygen atoms and the acidic bipyridinium hydrogen atoms—are responsible for these self-assembly processes. This synthetic methodology can be employed to self-assemble the mono- and bisfunctionalized [2]-catenanes depicted in Figure 2. The monofunctionalized

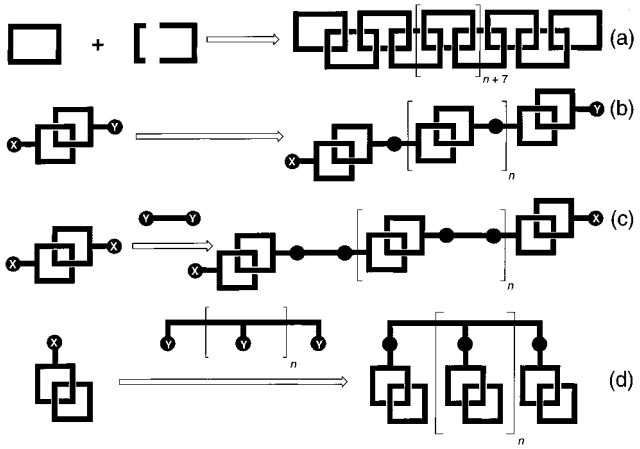

Figure 1. Schematic representation of (a−c) main-chain and (d) side-chain polycatenanes.

* Address correspondence to this author: Department of Chemistry and Biochemistry, University of California at Los Angeles, 405 Hilgard Avenue, Los Angeles, California 90095-1569.

† Molecular Meccano. 25. Part 24: Ashton, P. R.; Fyfe, M. C. T.; Glink, P. T.; Menzer, S.; Stoddart, J. F.; White, A. J. P.; Williams, D. J. *J. Am. Chem. Soc.* **1997**, *119*, 12514−12524.

S0024-9297(97)00685-2 CCC: $15.00
Published on Web 01/06/1998

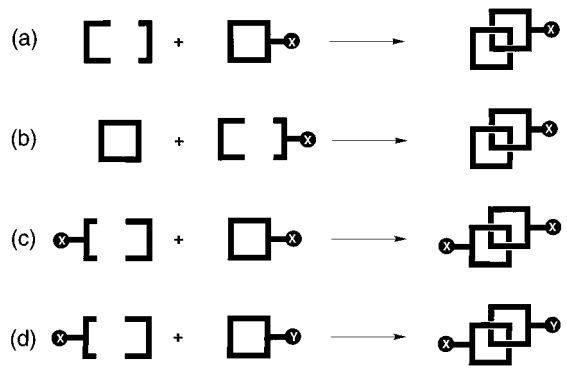

Figure 2. Schematic representation of the synthetic strategy adopted to self-assemble (a and b) mono- and (c and d) difunctionalized catenanes.

[2]catenanes can be prepared by (Figure 2a) the macrocyclization of the nonfunctionalized macrocycle around the functionalized one or by (Figure 2b) the introduction of the functional group during the macrocyclization step. By a combination of the two approaches, difunctionalized [2]catenanes incorporating identical and different (Figure 2c,d, respectively) functional groups on each macrocyclic component can also be produced.

Here, we report the self-assembly and the characterization of a series of mono- and difunctionalized [2]catenanes matching those depicted schematically in Figure 2. In addition, the synthesis of an oligo[2]catenane incorporating 17 monomeric [2]catenane repeating units, achieved according to the general route outlined in Figure 1c, is also described.

Experimental Section

General Methods. Chemicals were purchased from Aldrich and used as received. DMF and MeCN were distilled from CaH_2 and Me_2CO was distilled from molecular sieves (3 Å) according to procedures described in the literature.[11] The compounds **1**,[7e] **2**,[12] **5**·2PF_6,[7a] **6**,[7a] **7**,[13] and **12**[14] were prepared according to literature procedures. Thin layer chromatography (TLC) was carried out using aluminum sheets precoated with silica gel 60 F (Merck 5554). The plates were inspected by UV light and developed with iodine vapor or treated with either ethanolic ammonium thiocyanate or ceric ammonium molybdate. Column chromatography was carried out using silica gel 60 F (Merck 9385, 230−400 mesh). Gel permeation chromatography was carried out on a 420 Kontrun HPLC instrument equipped with a Knauer Differential Refractometer No 98. Aqueous NaCl (1 M) was employed as the eluant (flow rate 0.5 mL min^{-1}) in conjunction with a Sephadex G-75 column (length 100 cm, diameter 1 cm) calibrated using ribonuclease A (13.7 kg mol^{-1}), chymotrypsinogen A (25.0 kg mol^{-1}), ovalbumin (43.0 kg mol^{-1}), albumin (67.0 kg mol^{-1}), blue dextran 2000 (300.0 kg mol^{-1}), and lactose (180 g mol^{-1}) as standards.[15] Infrared spectra were recorded on a Paragon 1000 Perkin-Elmer FTIR spectrometer using a Nujol mull and NaCl disks. Melting points were determined on an Electrothermal 9200 apparatus and are not corrected. Electron impact mass spectra (EIMS) were recorded on a Kratos Profile spectrometer. Liquid secondary ion mass spectra (LSIMS) were obtained from a VG Zabspec mass spectrometer, equipped with a 35 keV cesium ion gun. Samples were dissolved in either a 3-nitrobenzyl alcohol or 2-nitrophenyl octyl ether matrix, previously coated onto a stainless steel probe tip. ^{1}H-NMR spectra were recorded on either a Bruker AC300 (300 MHz) or a Bruker AMX400 (400 MHz) spectrometer, using either the solvent or TMS as internal standards. ^{13}C-NMR spectra were recorded on either a Bruker AC300 (75.5 MHz) spectrometer or a Bruker AMX400 (100.6 MHz) spectrometer, using either the solvent or TMS as internal standards. All chemical shifts are quoted in ppm on the δ scale and the coupling constants are expressed in hertz (Hz).

1,4,7,10,13,20,23,26,29,32-Decaoxa[13,13]-[1,5-naphtho]-[1,3-(5-carbomethoxy)benzo]phane (3). Cesium tosylate (0.4 g, 1 mmol) and cesium carbonate (2.9 g, 6 mmol) were dissolved in dry DMF (1.3 L). After the temperature was raised up to 125 °C, a solution of methyl 3,5-dihydroxybenzoate (**2**) (1.0 g, 6 mmol) and 1,5-bis[2-[2-[2-(2-bromoethoxy)ethoxy]-ethoxy]ethoxy]naphthalene (**1**) (4.6 g, 6 mmol) in dried DMF (0.6 L) was added over 72 h. After cooling down to room temperature, the reaction mixture was filtered, and the filtrate was concentrated under reduced pressure. Purification of the resulting brown oil by column chromatography (SiO_2, $MeCO_2$-Et) gave **3** (1.3 g, 35%) as a yellow oil. LSIMS: m/z 644 $[M]^+$. ^{1}H-NMR ($CDCl_3$): δ 3.51−4.04 (31H, m), 4.18−4.21 (4H, t, J = 5 Hz), 6.50−6.53 (1H, m), 6.70−6.73 (2H, m), 7.08−7.11 (2H, m), 7.20−7.23 (2H, m), 7.80−7.83 (2H, m). ^{13}C-NMR ($CDCl_3$): δ 52.1, 67.7, 68.2, 69.5, 69.8, 70.8, 70.9, 70.9, 71.1, 105.8, 106.4, 108.1, 114.7, 125.1, 126.9, 131.7, 154.4, 159.8. Anal. ($C_{34}H_{44}O_{12}$) Calcd: C, 63.35; H, 6.83. Found: C, 63.21; H, 6.78.

1,4,7,10,13,20,23,26,29,32-Decaoxa[13,13]-[1,5-naphtho]-[1,3-(5-carboxy)benzo]phane (4). A solution of **3** (3.4 g, 5 mmol) in 2M NaOH (20 mL) and glycerol (20 mL) was heated to 120 °C over 24 h. After cooling down to room temperature, the solution was neutralized with 5 M HCl (10 mL) and extracted with CH_2Cl_2 (3 × 50 mL). The combined organic layers were washed with brine (3 × 50 mL), dried ($MgSO_4$), and concentrated under reduced pressure to afford **4** (2.8 g, 85%) as a white solid, mp 113−114 °C. LSIMS m/z 630 $[M]^+$. ^{1}H-NMR ($CDCl_3$): δ 3.60−3.78 (16H, m), 3.80−3.82 (4H, t, J = 5 Hz), 3.85−3.87 (4H, t, J = 5 Hz),4.00−4.02 (4H, t, J = 5 Hz), 4.26 (4H, t, J = 5 Hz), 6.40−6.44 (1H, m), 6.72−6.75 (2H, m), 7.15−7.18 (2H, m), 7.40−7.43 (2H, m), 7.80−7.84 (2H, m). ^{13}C-NMR ($CDCl_3$): δ 63.71, 67.67, 68.12, 69.53, 69.75, 70.85, 70.96, 71.05, 105.73, 106.95, 108.51, 114.63, 125.13, 126.71, 132.10, 154.32, 159.72, 170.31. Anal. ($C_{33}H_{42}O_{12}$) Calcd: C, 62.85; H, 6.71. Found: C, 62.54; H, 6.52.

3,5-Bis(bromomethyl)(hydroxymethyl)benzene (8). 1,3,5-Tris(hydroxymethyl)benzene (50 g, 170 mmol) and carbon tetrabromide (200 g, 610 mmol) were added to stirring THF (0.5 L); the triol did not dissolve fully but remained as a suspension. Ph_3P (160 g, 610 mmol) was added in portions over 10 min, while the reaction mixture was cooled with an ice-bath to maintain the temperature below 30 °C. The mixture was stirred at ambient temperature for a further 30 min, and then the solvent was removed under reduced pressure. The resulting solid was treated with PhMe (1.5 L) and then with hexane (1.0 L). After filtration, the resulting solution was concentrated under reduced pressure and allowed to stand until Ph_3PO had crystallized out. The mixture was filtered and the solid was washed with PhMe (2 × 50 mL). The combined solutions were concentrated on a rotary evaporator and the resulting residue purified by column chromatography (SiO_2, CH_2Cl_2) to give **8** (37 g, 43%) as a white crystalline solid, mp 64 °C. EIMS: m/z 294 $[M]^+$. ^{1}H-NMR ($CDCl_3$): δ 1.71−1.78 (1H, m), 4.48 (4H, s), 4.68 (2H, d, J = 5 Hz), 7.45 (3H, s). ^{13}C-NMR ($CDCl_3$): δ 32.6, 64.6, 127.4, 128.8, 138.8, 142.3. Anal. ($C_9H_{11}OBr_2$) Calcd: C, 36.73; H, 3.74. Found: C, 36.82; H, 3.60.

General Procedures for the Synthesis of the [2]Catenanes. Method A. A solution of the bis(hexafluorophosphate) salt **5**·2PF_6 (555 mg, 0.8 mmol), either the dibromide **7** or **8** (0.8 mmol), and each of the macrocyclic polyethers **4**, **6**, or **12** (1.6 mmol) in turn dissolved dry DMF (10 mL) was subjected to a pressure of 12 kbar at 20 °C for 3 d. The solvent was removed under reduced pressure and the residue purified by column chromatography (SiO_2, MeOH/2M NH_4Cl_{aq}/$MeNO_2$, 7:2:1) to afford reddish-purple solids which were dissolved in H_2O. After the addition of NH_4PF_6 to the reddish-purple solutions, the corresponding [2]catenanes precipitated out of the solutions as reddish-purple crystalline solids.

[2]Catenane 9·4PF_6. Yield = 15%; mp > 250 °C. LSIMS: m/z 1535 $[M - PF_6]^+$, 1390 $[M - 2PF_6]^+$, 1245 $[M - 3PF_6]^+$. ^{1}H-NMR (CD_3CN): δ 3.29 (4H, s), 3.50−3.90 (32H, m), 5.66 (4H, s), 5.82 (4H, s), 6.17 (4H, s), 7.64 (4H, d, J = 7 Hz), 7.69 (4H, d, J = 7 Hz), 7.75 (4H, s), 7.82 (1H, s), 8.57 (2H, s), 8.71

(4H, d, J = 7 Hz), 8.82 (4H, d, J = 7 Hz). ^{13}C-NMR (CD_3CN): δ 64.6, 65.7, 67.3, 68.6, 70.5, 71.2, 116.1, 118.3, 118.9, 126.0, 126.4, 132.0, 133.4, 134.5, 134.8, 135.2, 145.5, 146.3, 146.6, 152.9, 160.3. Anal. ($C_{65}H_{72}F_{24}N_4O_{12}P_4$) Calcd: C, 46.42; H, 4.28; N, 3.33. Found: C, 46.47; H, 4.17; N, 3.30.

[2]Catenane 10·4PF$_6$. Yield = 15%; mp > 250 °C. LSIMS: m/z 1666 $[M]^+$, 1521 $[M - PF_6]^+$, 1376 $[M - 2PF_6]^+$, 1231 $[M - 3PF_6]^+$. ^{1}H-NMR (CD_3CN): δ 3.29 (4H, s), 3.69−3.76 (8H, m), 3.79−3.98 (24H, m), 4.86 (1H, s), 5.36 (2H, s), 5.69 (4H, s), 5.79 (4H, s), 6.21 (4H, s), 7.59 (1H, s), 7.66−7.76 (8H, m), 7.79 (4H, s), 7.93 (2H, s), 8.74 (4H, d, J = 7 Hz), 8.96 (4H, d, J = 7 Hz). ^{13}C-NMR (CD_3CN): δ 63.6, 64.9, 65.1, 65.3, 65.6, 67.1, 68.4, 70.4, 71.0, 71.1, 71.3, 114.1, 115.9, 125.9, 126.2, 131.8, 132.4, 133.4, 134.5, 134.8, 137.4, 141.2, 145.3, 146.1, 146.5, 151.0, 152.9. Anal. ($C_{65}H_{74}F_{24}N_4O_{11}P_4$) Calcd: C, 46.81; H, 4.40; N, 3.36. Found: C, 46.73; H, 4.32; N, 3.35.

[2]Catenane 15·4PF$_6$. Yield = 24%; mp > 250 °C. LSIMS: m/z 1629 $[M - PF_6]^+$, 1484 $[M - 2PF_6]^+$, 1339 $[M - 3PF_6]^+$. ^{1}H-NMR (CD_3CN): δ 2.37−2.40 (2H, m), 3.20−4.45 (32H, m), 5.64−6.08 (9H, m), 6.29−6.32 (2H, m), 6.89−7.25 (10H, m), 7.60−7.64 (2H, m), 7.96−8.08 (5H, m), 8.30 (2H, d, J = 7 Hz), 8.60−8.64 (2H, m), 8.74 (2H, d, J = 7 Hz), 8.85 (2H, d, J = 7 Hz), 9.08 (2H, d, J = 7 Hz). ^{13}C-NMR (CD_3CN): δ 64.4, 65.2, 66.1, 68.5, 68.7, 68.9, 69.4, 70.4, 70.5, 70.6, 70.6, 70.7, 71.4, 71.6, 71.9, 99.9, 105.1, 105.6, 106.8, 107.2, 109.6, 110.8, 125.4, 126.5, 126.9, 127.8, 129.7, 132.3, 132.6, 134.9, 135.9, 137.6, 137.8, 138.0, 139.9, 145.2, 145.5, 146.1, 146.6, 160.4, 166.6. Anal. ($C_{70}H_{74}F_{24}N_4O_{14}P_4$) Calcd: C, 47.35; H, 4.17; N, 3.04. Found: C, 47.28; H, 4.10; N, 3.10.

[2]Catenane 16·4PF$_6$. Yield = 22%; mp > 250 °C. LSIMS: m/z 1760 $[M]^+$, 1615 $[M - PF_6]^+$, 1470 $[M - 2PF_6]^+$, 1325 $[M - 3PF_6]^+$. ^{1}H-NMR (CD_3CN): δ 2.27−2.30 (2H, m), 3.10−4.50 (34H, m), 5.30 (1H, s) 5.64−6.24 (8H, m), 6.29−6.32 (2H, m), 6.89−6.92 (2H, m), 7.01−7.18 (4H, m), 7.42−7.72 (6H, m), 7.82−7.85 (2H, m), 7.98−8.01 (3H, m), 8.40 (2H, d, J = 7 Hz), 8.50−8.53 (2H, m), 8.72 (2H, d, J = 7 Hz), 8.80 (2H, d, J = 7 Hz), 9.02 (2H, d, J = 7 Hz). ^{13}C-NMR (CD_3CN): δ 64.5, 65.2, 66.1, 68.5, 68.7, 69.0, 70.6, 70.7, 71.1, 71.2, 71.3, 71.4, 71.5, 71.6, 71.9, 105.0, 105.6, 105.7, 106.7, 107.2, 107.3, 109.6, 109.6, 109.7, 110.7, 110.9, 110.9, 125.4, 126.6, 126.9, 127.8, 129.7, 132.3, 132.5, 134.9, 135.2, 136.0, 137.6, 145.5, 145.8, 146.5, 166.7. Anal. ($C_{70}H_{76}F_{24}N_4O_{13}P_4$) Calcd: C, 47.72; H, 4.32; N, 3.18. Found: C, 47.60; H, 4.29; N, 3.15.

[2]Catenane 17·4PF$_6$. Yield = 20%; mp > 250 °C. LSIMS: m/z 1760 $[M]^+$, 1615 $[M - PF_6]^+$, 1470 $[M - 2PF_6]^+$, 1325 $[M - 3PF_6]^+$. ^{1}H-NMR (CD_3CN): δ 2.40−2.43 (2H, m), 3.10−4.40 (32H, m), 4.90−4.93 (2H, m), 5.51−5.53 (1H, m), 5.65−6.10 (10H, m), 6.25−6.28 (2H, m), 6.70−6.73 (2H, m), 6.92−6.94 (2H, m), 7.09−7.20 (8H, m), 7.71−7.73 (1H, m), 7.84−7.86 (2H, m), 8.00−8.03 (4H, m), 8.25 (2H,d, J = 7 Hz), 8.50−8.54 (2H, m), 8.85 (2H, d, J = 7 Hz), 9.08 (2H, d, J = 7 Hz). ^{13}C-NMR (CD_3CN): δ 63.6, 65.6, 65.9, 68.7, 68.8, 69.0, 69.2, 70.1, 70.4, 70.8, 70.9, 71.2, 71.5, 71.7, 104.9, 105.5, 106.0, 109.3, 109.7, 110.9, 125.0, 125.3, 126.3, 126.8, 127.7, 129.4, 132.1, 132.2, 132.4, 132.7, 133.2, 134.3, 137.4, 145.2, 145.4, 145.7, 146.4, 146.6, 146.9. Anal. ($C_{70}H_{76}F_{24}N_4O_{13}P_4$) Calcd: C, 47.72; H, 4.32; N, 3.18. Found: C, 47.67; H, 4.40; N, 3.18.

[2]Catenane 18·4PF$_6$. Yield = 18%; mp > 250 °C. LSIMS: m/z 1746 $[M]^+$, 1601 $[M - PF_6]^+$, 1456 $[M - 2PF_6]^+$, 1312 $[M - 3PF_6]^+$; ^{1}H-NMR (CD_3CN): δ 2.40−2.43 (2H, m), 3.18−3.21 (2H, m), 3.25−3.27 (2H, m), 3.40−3.44 (4H, m), 3.50−4.50 (26H, m), 4.90−4.94 (2H, m), 5.23−5.25 (1H, m), 5.61−6.30 (12H, m), 6.95−6.98 (2H, m), 7.03−7.17 (8H, m), 7.77−7.79 (2H, m), 7.84−7.86 (2H, m), 8.00−8.03 (5H, m), 8.40 (2H, d, J = 7 Hz), 8.55 (2H, d, J = 7 Hz), 8.90 (2H, d, J = 7 Hz), 9.08 (2H, d, J = 7 Hz). ^{13}C-NMR (CD_3CN): δ 63.8, 64.5, 65.8, 66.1, 68.5, 68.7, 68.9, 69.3, 70.5, 71.3, 71.4, 71.6, 71.6, 71.9, 71.9, 99.7, 104.9, 105.5, 106.7, 107.2, 109.6, 111.2, 125.1, 125.3, 126.5, 126.8, 128.0, 129.6, 132.3, 132.6, 132.8, 134.4, 137.6, 145.2, 145.5, 145.6, 145.9, 146.5. Anal. ($C_{70}H_{78}F_{24}N_4O_{12}P_4$) Calcd: C, 48.10; H, 4.46; N, 3.20. Found: C, 47.97; H, 4.59; N, 3.14.

Method B. A solution of the bis(hexafluorophosphate) salt **5**·2PF$_6$ (433 mg, 0.6 mmol), the dibromide **11** (162 mg, 0.6 mmol), and either the macrocyclic polyether **4** or **12** (1.2 mmol) in dry DMF (8 mL) was stirred at room temperature for 14 d. The solvent was removed under reduced pressure and the residue purified by column chromatography (SiO_2, MeOH/2 M NH_4Cl_{aq}/$MeNO_2$, 7:2:1) to afford reddish-purple solids which were dissolved in H_2O. After the addition of NH_4PF_6 to the reddish-purple solutions, the [2]catenanes precipitated out of the solution as reddish-purple crystalline solids.

[2]Catenane 13·4PF$_6$. Yield = 34%; mp > 250 °C. LSIMS: m/z 1730 $[M]^+$, 1585 $[M - PF_6]^+$, 1440 $[M - 2PF_6]^+$, 1180 $[M - 3PF_6]^+$. ^{1}H-NMR (CD_3CN): δ 2.40−2.43 (2H, m), 3.38−3.39 (4H, m), 3.50−3.53 (4H, m), 3.67−3.70 (4H, m), 3.88−3.90 (4H, m), 3.96−3.99 (4H, m), 4.06−4.09 (4H, m), 4.19−4.22 (4H, m), 4.29−4.32 (4H, m), 5.53−5.57 (1H, m), 5.71 (4H, d, J = 8 Hz), 5.78 (4H, d, J = 8 Hz), 5.92−5.95 (2H, m), 6.20−6.23 (2H, m), 6.30−6.33 (2H, m) 7.10 (8H, 4H, d, J = 7 Hz), 7.95−7.97 (4H, m), 8.07−8.09 (4H, m), 8.52 (4H, 4H, d, J = 7 Hz), 9.02 (4H, 4H, d, J = 7 Hz). ^{13}C-NMR (CD_3CN): δ 66.1, 69.3, 70.6, 71.0, 71.7, 71.8, 72.3, 105.3, 109.4, 109.6, 118.5, 125.6, 126.6, 129.4, 132.3, 132.6, 137.6, 145.6, 145.8, 152.2, 160.6. Anal. ($C_{69}H_{74}F_{24}N_4O_{12}P_4$) Calcd: C, 47.86; H, 4.39; N, 3.23. Found: C, 47.61; H, 4.52; N, 3.53.

[2]Catenane 14·4PF$_6$. Yield = 23%; mp > 250 °C. LSIMS: m/z 1716 $[M]^+$, 1572 $[M - PF_6]^+$, 1427 $[M - 2PF_6]^+$, 1282 $[M - 3PF_6]^+$. ^{1}H-NMR (CD_3CN): δ 2.40−2.43 (2H, m), 3.28−3.30 (4H, m), 3.40−3.43 (4H, m), 3.62−3.65 (4H, m), 3.80−3.83 (4H, m), 3.99−4.02 (4H, m), 4.06−4.09 (4H, m), 4.19−4.23 (4H, m), 4.29−4.32 (4H, m), 4.49 (2H, bs), 5.23−5.25 (1H, m), 5.71 (4H, d, J = 8 Hz), 5.78 (4H, d, J = 8 Hz), 5.92−5.95 (2H, m), 6.20−6.23 (4H, m), 7.10 (8H, d, J = 7 Hz), 7.95−7.98 (4H, m), 8.07−8.08 (4H, m), 8.52 (4H, d, J = 7 Hz), 9.02 (8H, d, J = 7 Hz). ^{13}C-NMR (CD_3CN): δ 64.4, 66.0, 68.7, 69.3, 70.5, 70.7, 71.6, 71.7, 72.1, 99.9, 105.1, 107.0, 109.3, 125.3, 126.4, 129.2, 132.1, 132.4, 137.6, 145.5, 146.0, 146.2, 152.1, 160.6. Anal. ($C_{69}H_{76}F_{24}N_4O_{11}P_4$) Calcd: C, 48.25; H, 4.42; N, 3.26. Found: C, 48.06; H, 4.49; N, 3.15.

X-ray Crystallography. The crystal data, data collection, and refinement parameters for the [2]catenanes **10**·4PF$_6$, **13**·4PF$_6$, **14**·4PF$_6$, and **17**·4PF$_6$ are summarized in Table 1. All four structures were solved by direct methods and were refined by full-matrix least-squares methods based on F^2. In all cases, the tetracationic cyclophane components were ordered and of full occupancy. In **10**·4PF$_6$, **13**·4PF$_6$, and **17**·4PF$_6$, the tetracationic cyclophane component was treated anisotropically while **14**·4PF$_6$ was refined isotropically as a result of a shortage of observed data and because such cyclophanes seldom exhibit significant anisotropy. The macrocyclic polyether components of **10**·4PF$_6$ and **13**·4PF$_6$ were ordered and were refined anisotropically. In **14**·4PF$_6$, the oxygen atom of the hydroxymethyl substituent of the macrocyclic polyether was disordered over two partial occupancy sites (75:25); the minor occupancy atom was refined isotropically, and the remainder of the atoms were refined anisotropically. In **17**·4PF$_6$, the macrocyclic polyether exhibited significant disorder in one of the polyether chains, and this was resolved into two 50:50 orientations, both of which were refined isotropically; the remaining full occupancy atoms were refined anisotropically. In all four structures, there was found to be a mixture of both full and partial occupancy ordered and disordered hexafluorophosphate counterions. In all cases, the major occupancy atoms were refined anisotropically, while the minor occupancy atoms were also treated anisotropically for **13**·4PF$_6$. In **10**·4PF$_6$, portions of the [2]catenane and the hexafluorophosphate counterions were refined as optimized rigid bodies, as a result of a severe shortage of observed data. The ordered and disordered full and partial occupancy included solvent molecules in each structure were treated partially anisotropically and partially isotropically. In all four structures, the C−H hydrogen atoms of the [2]catenanes were placed in calculated positions, assigned isotropic thermal parameters, $U(H) = 1.2U_{eq}(C)$, and allowed to ride on their parent atoms. The positions of the hydrogen atoms of the included solvent molecules and of the hydroxyl groups of the [2]catenanes could not be reliably located or calculated. Computations were carried out using the SHELXTL PC program system[16] and XtalView 3.1.[17]

Table 1. Crystal Data, Data Collection and Refinement Parameters for the [2]Catenanes 10·4PF$_6$, 13·4PF$_6$, 14·4PF$_6$, and 17·4PF$_6$[a]

data	**10**·4PF$_6$	**13**·4PF$_6$	**14**·4PF$_6$	**17**·4PF$_6$
formula	$C_{65}H_{74}N_4O_{11}$·4PF$_6$	$C_{69}H_{74}N_4O_{12}$·4PF$_6$	$C_{69}H_{76}N_4O_{11}$·4PF$_6$	$C_{70}H_{76}N_4O_{13}$·4PF$_6$
solvent	PhH·MeCN·0.5MeOH	6MeCN·0.5H_2O	7MeCN	8MeCN
fw	1802.3	1986.5	2004.6	2090.2
color, habit	red plates	red platy needles	orange plates	red blocks
cryst size (mm)	0.33 × 0.17 × 0.07	0.30 × 0.20 × 0.13	0.73 × 0.50 × 0.10	0.50 × 0.24 × 0.24
lattice type	triclinic	triclinic	monoclinic	triclinic
space group symbol, no.	$P\bar{1}$, 2	$P\bar{1}$, 2	$P2_1/c$, 14	$P\bar{1}$, 2
T (K)	203	193	293	203
cell dimens				
a (Å)	13.787(2)	13.683(2)	13.752(2)	14.367(3)
b (Å)	16.210(5)	13.942(3)	25.952(2)	17.023(2)
c (Å)	20.869(9)	27.228(6)	27.314(3)	21.631(2)
α (deg)	104.57(3)	77.88(1)		91.81(1)
β (deg)	102.60(2)	85.09(1)	93.11(2)	102.03(1)
γ (deg)	106.37(2)	74.11(3)		94.85(2)
V (Å^3)	4116(2)	4882(2)	9734(2)	5149(1)
Z	2	2	4	2
D_c (g cm^{-3})	1.453	1.351	1.368	1.348
F(000)	1858	2050	4144	2161
μ (mm^{-1})	1.87	1.65	1.65	1.60
θ range (deg)	2.3−55.0	1.7−55.0	2.4−55.0	2.6−55.0
no. of unique reflcns				
measd	8996	12235	12034	12718
obsd, $\|F_o\| > 4\sigma(\|F_o\|)$	3761	7886	5494	8791
no. of variables	924	1263	970	1314
R_1[b]	0.189	0.125	0.120	0.090
wR_2[c]	0.467	0.333	0.308	0.249
weighting factors a, b[d]	0.407, 2.353	0.277, 3.638	0.201, 37.588	0.180, 5.228
largest difference peak, hole (e Å^{-3})	1.07, −0.75	0.98, −0.52	0.91, −0.53	0.73, −0.46

[a] Details in common: graphite-monochromated radiation, ω-scans, Siemens P4 rotating anode diffractometer, Cu Kα radiation, refinement based on F^2. [b] $R_1 = \Sigma||F_o| - |F_c||/\Sigma|F_o|$. [c] $wR_2 = \sqrt{\{\Sigma[w(F_o^2 - F_c^2)^2]/\Sigma[w(F_o^2)^2]\}}$. [d] $w^{-1} = \sigma^2(F_o^2) + (aP)^2 + bP$.

Attempted Polyesterifications. Method A. Diisopropylcarbodiimide (4 mmol) was added to a solution of 4-(dimethylamino)pyridinium 4-toluenesulfonate (0.3 mmol) and one of the [2]catenanes, **15**·4PF$_6$, **16**·4PF$_6$, or **17**·4PF$_6$, or terephthalic acid (0.15 mmol) in MeCN, Me_2CO, or DMF (3 mL). In the case of the diacids, after the reaction was stirred at room temperature for 30 min, the corresponding diol—*i.e.*, hydroquinone in the case of **15**·4PF$_6$ and the [2]catenane **18**·4PF$_6$ in the case of terephthalic acid—(0.15 mmol) was added to the solution. After 3 days, *t*-BuN_4Cl was added to the reaction mixture to afford a purple precipitate which was filtered off and washed with Me_2CO and dissolved in H_2O. Addition of an excess of KPF$_6$ gave a purple precipitate corresponding to the *N*-acyl derivative of the original [2]catenane containing (a) carboxylic acid function(s) or corresponding to the unreacted [2]catenane in the case of the dihydroxymethyl[2]catenane **18**·4PF$_6$.

Method B. *N*,*N*′-Bis(2-oxo-3-oxazolidinyl)phosphorodiamic chloride (0.3 mmol) was added to a solution of lutidine (0.3 mmol) and one of the [2]catenanes, **15**·4PF$_6$, **16**·4PF$_6$, or **17**·4PF$_6$, or terephthalic acid (0.15 mmol) in MeCN, Me_2CO, or DMF (3 mL). In the case of the diacids, after the reaction was stirred at room temperature for 30 min, the corresponding diol—*i.e.*, hydroquinone in the case of **15**·4PF$_6$ and the [2]catenane **18**·4PF$_6$ in the case of terephthalic acid—(0.15 mmol) was added to the solution. After 3 days, *t*-BuN_4Cl was added to the reaction mixture to afford a purple precipitate which was filtered off and washed with Me_2CO and dissolved in H_2O. Addition of an excess of KPF$_6$ gave a purple precipitate corresponding to the unreacted [2]catenane.

Method C. 1,2-Benzisooxazol-3-yl diphenyl phosphate (0.3 mmol) was added to a solution of lutidine (0.3 mmol) and one of the [2]catenanes; **15**·4PF$_6$, **16**·4PF$_6$, or **17**·4PF$_6$, or terephthalic acid (0.15 mmol) in MeCN, Me_2CO, or DMF (3 mL). In the case of the diacids, after stirring at room temperature for 30 min, the corresponding diol—*i.e.*, hydroquinone in the case of **15**·4PF$_6$ and the [2]catenane **18**·4PF$_6$ in the case of terephthalic acid—(0.15 mmol) was added to the solution. After 3 days, *t*-BuN_4Cl was added to the reaction mixture to afford a purple precipitate which was filtered off and washed with Me_2CO and dissolved in H_2O. Addition of an excess of KPF$_6$ gave a purple precipitate corresponding to the unreacted [2]catenane.

Oligo[2]Catenane 19·4*n*PF$_6$. A solution of the [2]catenane **18**·4PF$_6$ (30.0 mg, 0.017 mmol) and bis(*p*-isocyanatophenyl)methane (4.28 mg, 0.017 mmol) in MeCN (5 mL) was heated under reflux for 2 days. After this cooled down to room temperature, *t*-BuN_4Cl was added to the reaction mixture, affording a purple precipitate. The resulting solid was filtered off and washed with Me_2CO and dissolved in H_2O. Addition of an excess of KPF$_6$ gave **19**·4*n*PF$_6$ (33 mg) as a purple precipitate, mp > 250 °C. ^{1}H-NMR (CD_3CN): δ 3.20−4.30 (32H, m), 4.90−5.00 (4H, m), 5.20 (2H, s), 5.50 (2H, s), 5.73 (6H, m), 5.88 (6H, m), 6.10−6.34 (5H, m), 6.90−7.40 (8H, m), 7.48−7.54 (6H, m), 7.77−7.82 (5H, m), 7.89−7.93 (4H, m), 8.40−9.20 (8H, m). ^{13}C-NMR (CD_3CN): δ 40.9, 65.4, 65.9, 66.4, 68.5, 68.8, 70.2, 71.2, 71.7, 99.9, 104.7, 105.3, 106.4, 109.4, 110.8, 118.2, 118.5, 119.8, 124.9, 125.1, 126.3, 127.8, 129.4, 130.12, 132.4, 133.1, 133.8, 134.5, 137.5, 145.3, 146.3, 151.9, 154.4, 154.8, 160.5. The purple solid was dissolved in MeCN, and *t*-Bu$_4$NCl was added to afford **19**·4*n*Cl as a purple precipitate. A small amount of **19**·4*n*Cl (10 mg) was dissolved in H_2O (1 mL) and the resulting solution was analysed by GPC employing the conditions described in the subsection on **General Methods**. The number-average molecular weight M_n was 26.5 kg mol^{-1}; the degree of polymerization based on M_n, was 17.

Results and Discussion

Synthesis of the Monomeric [2]catenanes. In order to self-assemble functionalized [2]catenanes, we have employed an approach involving the macrocyclization of a tetracationic bipyridinium-based macrocyclic component around an appropriate π-electron-rich macrocyclic polyether template. The potential lability of the resulting tetracationic cyclophane component to nucleophilic attack suggested the introduction, following the

Scheme 1

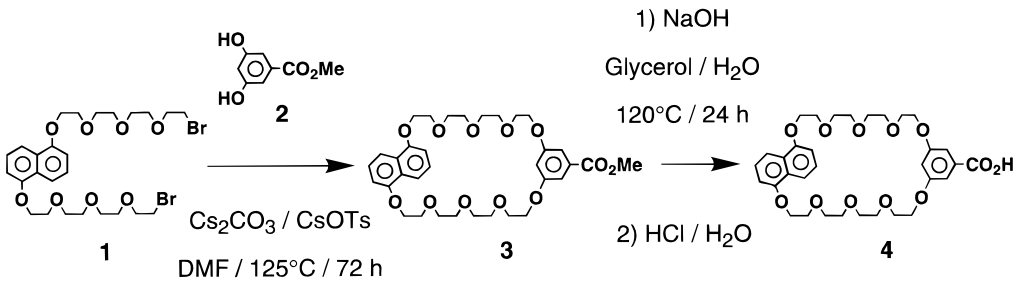

Scheme 2

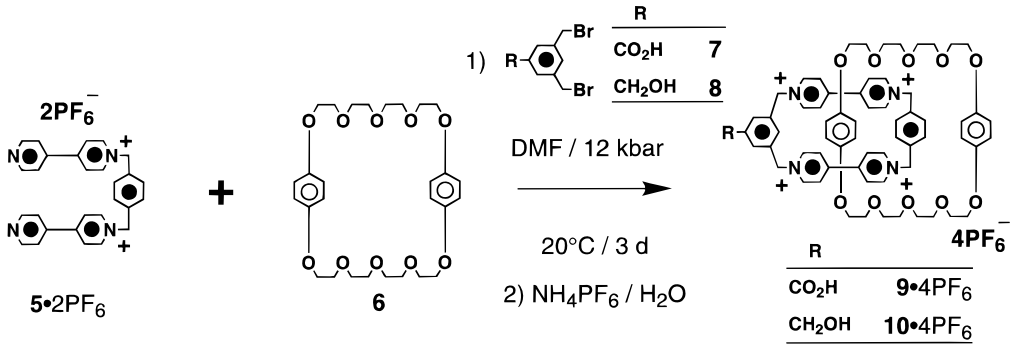

Scheme 3

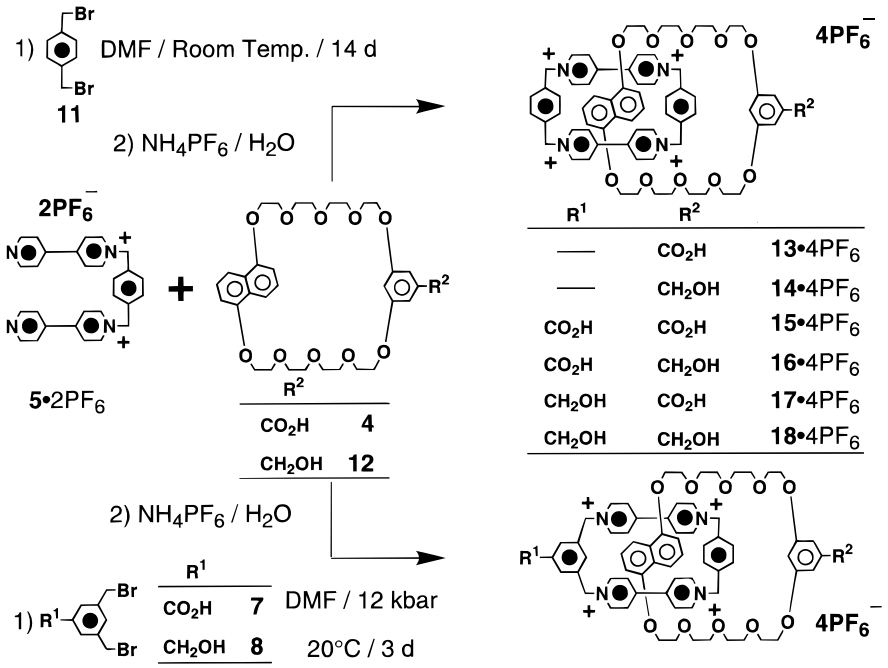

design logic illustrated in Figure 2, of hydroxyl and carboxyl groups as the reactive functionalities. These functionalities can then, in principle at least, be condensed under relatively mild conditions, thus preventing the degradation of the tetracationic component and—as a result—of the catenated structure. The macrocyclic polyethers **4** and **12**, as well as the dibromides **7** and **8** incorporating either a carboxylic acid function or a hydroxymethyl group, are suitable starting materials for the proposed syntheses. The preparation of the macrocycle **12**[14] and the dibromide **7**[13] have been reported in the literature previously, while the dibromide **8** was synthesized by bromination of 1,3,5-tris(hydroxymethyl)benzene. The π-electron rich macrocyclic polyether **4** was prepared as illustrated in Scheme 1. Reaction of the dibromide **1** with the diol **2** in the presence of cesium carbonate and cesium tosylate afforded the macrocycle **3** in a yield of 35%. Hydrolysis of the ester group was performed under basic conditions to give the macrocyclic polyether **4** in a yield of 85% after acidification.

The monofunctionalized [2]catenanes **9**·4PF_6 and **10**·4PF_6, incorporating a carboxylic acid function and a hydroxymethyl group, respectively, on the tetracationic cyclophane component were self-assembled using ultrahigh pressure conditions,[18] as depicted in Scheme 2. Reaction of the bis(hexafluorophosphate) salt **5**·2PF_6 with either **7** or **8** in the presence of the hydroquinone-based macrocyclic polyether **6** under 12 kbar at 20 °C during 3 days afforded the corresponding [2]catenanes

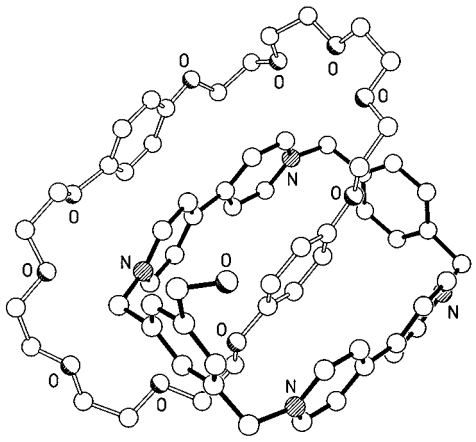

Figure 3. X-ray crystal structure of the monofunctionalized [2]catenane **10**·4PF_6.

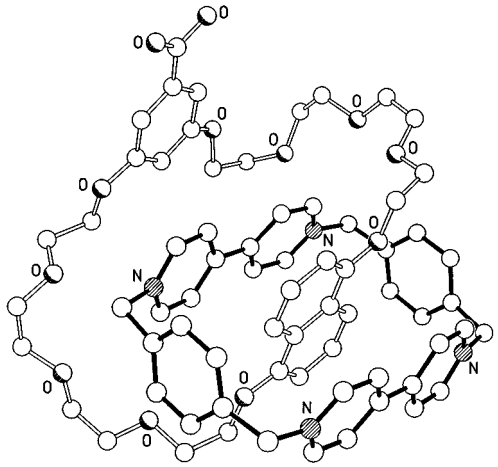

Figure 4. X-ray crystal structure of the monofunctionalized [2]catenane **13**·4PF_6.

9·4PF_6 or **10**·4PF_6, respectively, in yields of 15% in both instances.

The monofunctionalized [2]catenanes **13**·4PF_6 and **14**·4PF_6, incorporating a carboxylic acid function and a hydroxymethyl group, respectively, on the macrocyclic polyether component were self-assembled as depicted in Scheme 3. Reaction of the bis(hexafluorophosphate) salt **5**·2PF_6 with the dibromide **11** in the presence of either **4** or **12** at room temperature during 14 days afforded the corresponding [2]catenane **13**·4PF_6 or **14**·4PF_6, respectively, in yields of 34 and 23%. The difunctionalized [2]catenanes **15**·4PF_6 and **16**·4PF_6 incorporating a carboxylic acid function on the tetracationic cyclophane component and a carboxylic acid function or a hydroxymethyl group, respectively, on the macrocyclic polyether component were self-assembled under ultrahigh pressure conditions, as depicted in Scheme 3. Reaction of the bis(hexafluorophosphate) salt **5**·2PF_6 with the dibromide **7** in the presence of either **4** or **12**, under 12 kbar at 20 °C during 3 days, afforded the corresponding [2]catenane **15**·4PF_6 or **16**·4PF_6, respectively, in yields of 24 and 22%. The difunctionalized [2]catenanes **17**·4PF_6 and **18**·4PF_6, incorporating a hydroxymethyl group on the tetracationic cyclophane component, and a carboxylic acid function or a hydroxymethyl group, respectively, on the macrocyclic polyether component were self-assembled under ultrahigh pressure conditions, as depicted in Scheme 3. Reaction of the bis(hexafluorophosphate) salt **5**·2PF_6 with the dibromide **8** in the presence of either **4** or **12**, under 12 kbar at 20 °C during 3 days, afforded the corresponding [2]catenane **17**·4PF_6 or **18**·4PF_6, respectively, in yields of 20 and 18%.

X-ray Crystal Structures. The single-crystal X-ray analysis of the monofunctionalized [2]catenane **10**·4PF_6 is of limited accuracy as a result of severe disorder in the hexafluorophosphate counterions and a large number of poorly resolved included solvent molecules. However, the principal features of the [2]catenane **10**·4PF_6 are definitive. The only uncertainty is in the position of the hydroxymethyl oxygen atom attached to the tetracationic cyclophane component which appears to be freely rotating about the Ar−CH_2 bond, the only small maximum of electron density being at the position depicted in Figure 3. The geometry of the monofunctionalized [2]catenane **10**·4PF_6 is very similar to that observed[7c] for the nonfunctionalized analog and is stabilized (Table 2) by the usual combination of $\pi-\pi$ stacking, [C−H···O], and [C−H···π] interactions.

The single-crystal X-ray analysis of the monofunctionalized [2]catenane **13**·4PF_6 is illustrated in Figure 4. Whereas the 1,5-dioxynaphthalene ring is sandwiched symmetrically between the two bipyridinium

Table 2. Distances[a] (Å) and Angles[a] (deg) Characterizing the Molecular Geometries of the [2]Catenanes 10·4PF_6, 13·4PF_6, 14·4PF_6, and 17·4PF_6

compound	θ_i	θ_a	ψ_i	ψ_a	τ	$Z_i\cdots Z_a$	Y···Y′	$Z_a\cdots X_i$	$Z_i\cdots X_i$	$Z_i\cdots X_a$	H···Y	XHY	H′···Y′	H′XY′
10·4PF_6	7	6	30	29	43	6.94	10.52	3.47	3.46	3.44	2.76	160	3.16	180
13·4PF_6	11	6	21	20	52	6.73	10.44	3.35	3.37	3.43	2.54	149	2.54	145
14·4PF_6	10	4	24	24	53	6.87	10.38	3.44	3.42	3.47	2.53	149	2.51	149
17·4PF_6	18	9	27	23	54	6.70	10.63	3.36	3.33	3.67	3.15	120	2.49	147

[a] The distances and angles indicated in the table are illustrated in the diagrams A, B, and C. The subscripts a and i stand for alongside and inside, respectively.

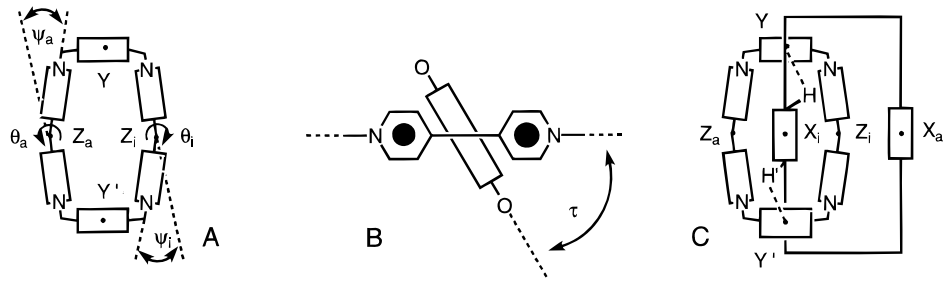

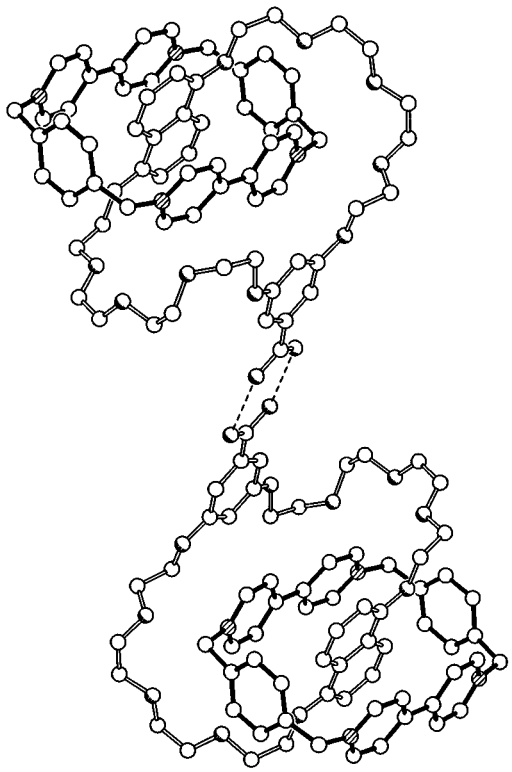

Figure 5. Hydrogen-bonded pairs of [2]catenanes formed by **13**·4PF_6 in the solid state.

units, the substituted resorcinol ring is displaced significantly above the mean plane of the tetracationic cyclophane. Thus, although the resorcinol ring is oriented parallel to the inside bipyridinium unit (mean interplanar separation of 3.43 Å), the degree of $\pi-\pi$ overlap is reduced substantially. The $\pi-\pi$ stacking interactions between the complementary aromatic units are again supplemented (Table 2) by weak intercomponent [C−H···O] hydrogen bonds and strong [C−H···π] interactions between the hydrogen atoms attached to positions 4 and 8 of the 1,5-dioxynaphthalene ring and the *p*-xylyl spacers of the tetracationic cyclophane. A surprising feature of the packing of the monofunctionalized [2]catenane **13**·4PF_6 is the absence of any extended π-stacked motifs. The only important intermolecular interaction is the formation (Figure 5) of hydrogen-bonded carboxylic acid "dimer pairs". Although the hydrogen atoms were not located, the 2.85 Å approach of both symmetry related oxygen atoms of the carboxylic acid functions is consistent with reasonable strength hydrogen bonds.

The X-ray crystal structure of the monofunctionalized [2]catenane **14**·4PF_6—the hydroxymethyl analog of **13**·4PF_6—exhibits (Figure 6) only minor conformational differences from **13**·4PF_6, these being in the geometries of the polyether linkages. The alongside substituted resorcinol ring is again oriented parallel to but offset with respect to the inside bipyridinium unit. The $\pi-\pi$, [C−H···O], and [C−H···π] stabilizing interactions (Table 2) are very similar to those observed in **13**·4PF_6. There is disorder in the orientation of the hydroxymethyl substituent with two principal orientations being observed. However, neither of these two positions are within hydrogen-bonding distance of any other ordered atoms in the structure, the closest contact of the principal occupancy site being to a disordered hexafluorophosphate counterion. Inspection of the packing of

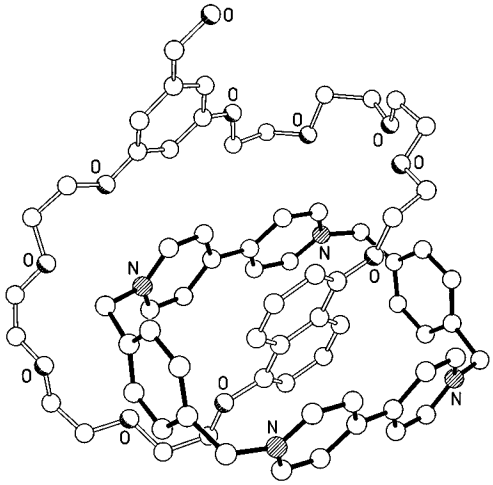

Figure 6. X-ray crystal structure of the monofunctionalized [2]catenane **14**·4PF_6.

the monofunctionalized [2]catenane **14**·4PF_6 reveals (Figure 7) the formation of a two-dimensional π-stacked mosaic. In one direction, the alongside bipyridinium unit of one [2]catenane overlays the substituted resorcinol ring of the next (mean interplanar separation 3.38 Å) whilst the *p*-xylyl rings of lattice translated molecules are stacked parallel to each other in the other direction (mean interplanar and centroid-centroid distances of 3.34 and 4.08 Å, respectively).

The single-crystal X-ray analysis of the difunctionalized [2]catenane **17**·4PF_6 reveals (Figure 8) a structure that retains features in common with **10**·4PF_6, **13**·4PF_6, and **14**·4PF_6. Indeed, the geometries of the polyether chains are virtually unchanged from that observed in **13**·4PF_6. Intercomponent stabilization include (Table 2) the usual spectrum of $\pi-\pi$, [C−H···O], and [C−H···π] interactions, though with the absence of a [C−H···π] interaction to the functionalized *m*-xylyl spacer, the [H···π] distance being 3.15 Å. The hydroxymethyl substituent on the *m*-xylyl spacer exhibits disorder with two positions being identified for the hydroxyl oxygen atom. In neither of these two positions is the oxygen atom within hydrogen bonding distance to any of the atoms within the [2]catenane or its symmetry-related counterparts. However, the major occupancy site lies only 2.85 Å from a fluorine atom of one of the hexafluorophosphate counterions, suggesting a possible [O−H···F] hydrogen bond. A search for anion−cation interactions revealed close approaches of two of the hydrogen atoms in the β-positions with respect to the nitrogen atoms on the bipyridinium units to fluorine atoms of an ordered hexafluorophosphate counterion ([H···F] and [C···F] distances and a [C−H···F] angle of 2.33 and 3.15 Å and 143°, respectively, in one instance and of 2.40 and 3.35 Å and 173°, respectively, in the other). The carboxylic acid function residing on the resorcinol ring forms a hydrogen bonded "dimer pair" with its C_i related counterpart in the crystal, the [O···O] separation being 2.63 Å. The packing of these "dimer pairs" is complex with both the *m*- and *p*-xylyl spacers of the tetracationic cyclophane components within each "dimer pair" π-stacked (mean interplanar and centroid−centroid separations of 3.45 and 3.65 Å, respectively, for the *m*-xyxlyl and 3.40 and 4.30 Å, respectively, for the *p*-xylyl spacers) with the C_i related counterparts in the crystal to form the sheet structure illustrated in Figure 9. Adjacent sheets normal to the plane of the paper are offset such that each of the substituted resorcinol rings

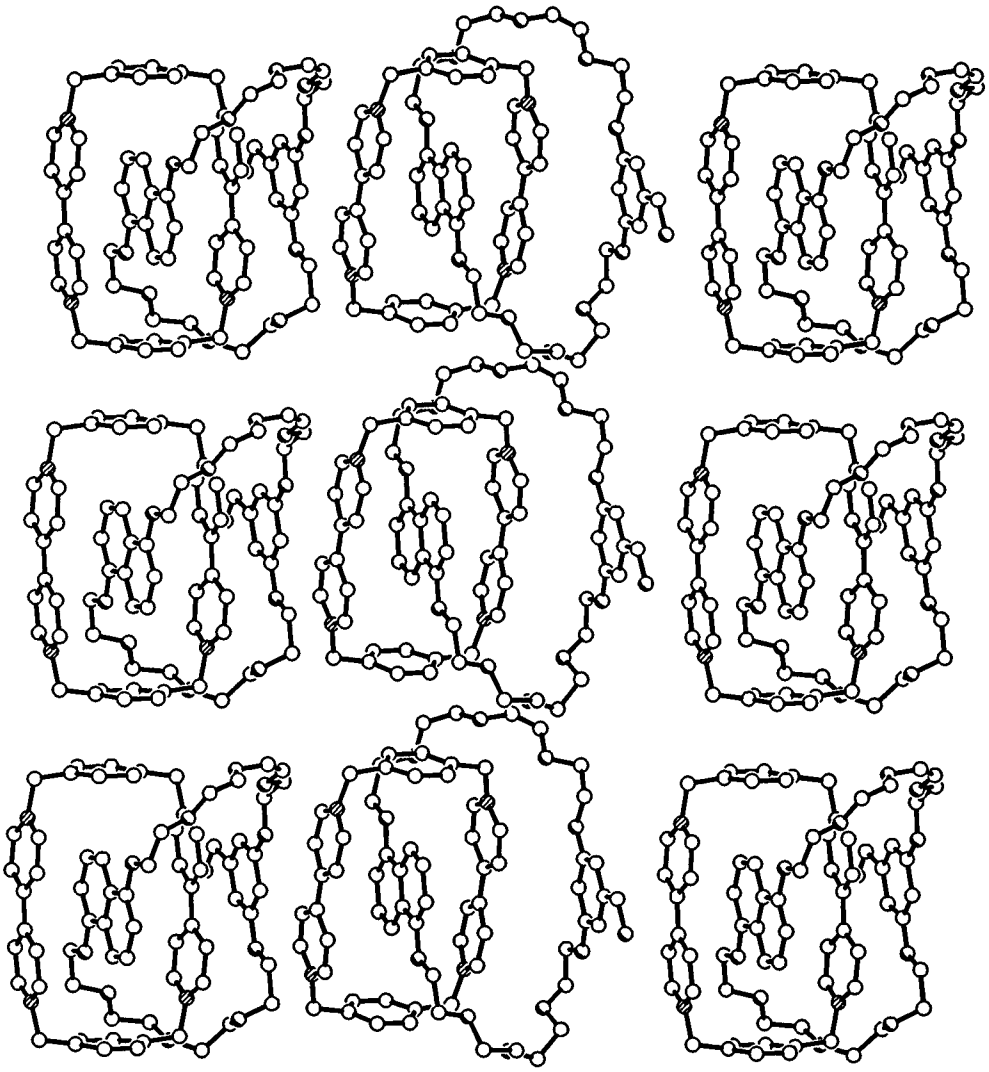

Figure 7. Packing diagram of the monofunctionalized [2]catenane **14**·4PF_6.

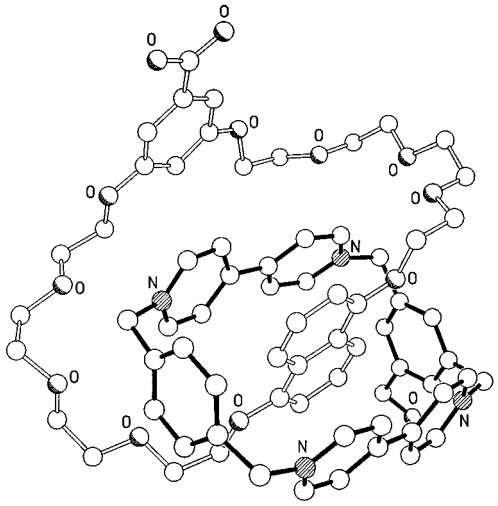

Figure 8. X-ray crystal structure of the difunctionalized [2]-catenane **17**·4PF_6.

in one sheet is π-stacked (Figure 10) with the alongside bipyridinium unit of the [2]catenane in the next and *vice versa* creating a continuous donor-acceptor sequence. The interplanar separation between the alongside substituted resorcinol ring in one layer and the alongside bipyridinium in the next is 3.31 Å.

^{1}H-NMR Spectroscopy. The dynamic processes illustrated schematically in Figure 11 are associated with the [2]catenanes **9**·4PF_6 and **10**·4PF_6, incorporating one functional group on their tetracationic cyclophane components, in solution, as demonstrated by variable temperature ^{1}H-NMR spectroscopic investigation. Process I involves the circumrotation of the macrocyclic polyether through the cavity of the tetracationic cyclophane. As a result of this process, the hydroquinone rings located *inside* and *alongside* the cavity of the tetracationic cyclophane component are undergoing exchange. Process II involves the circumrotation of the tetracationic cyclophane through the cavity of the macrocyclic polyether. However, the tetracationic cyclophane incorporates two different spacers separating the two bipyridinium units; thus, two different pathways can be envisaged for process II. Exchange of the *inside* and *alongside* bipyridinium units can occur after the passage of either the *p*-xylene or the *m*-xylene spacers through the cavity of the macrocyclic polyether component. Presumably, the passage of the bulkier *m*-xylene spacer is energetically more demanding. However, it is not possible to establish by variable temperature ^{1}H-NMR spectroscopy if process II is occurring by only one or both pathways. At room temperature, process I is slow on the ^{1}H-NMR time scale and the hydroquinone rings residing *alongside* and

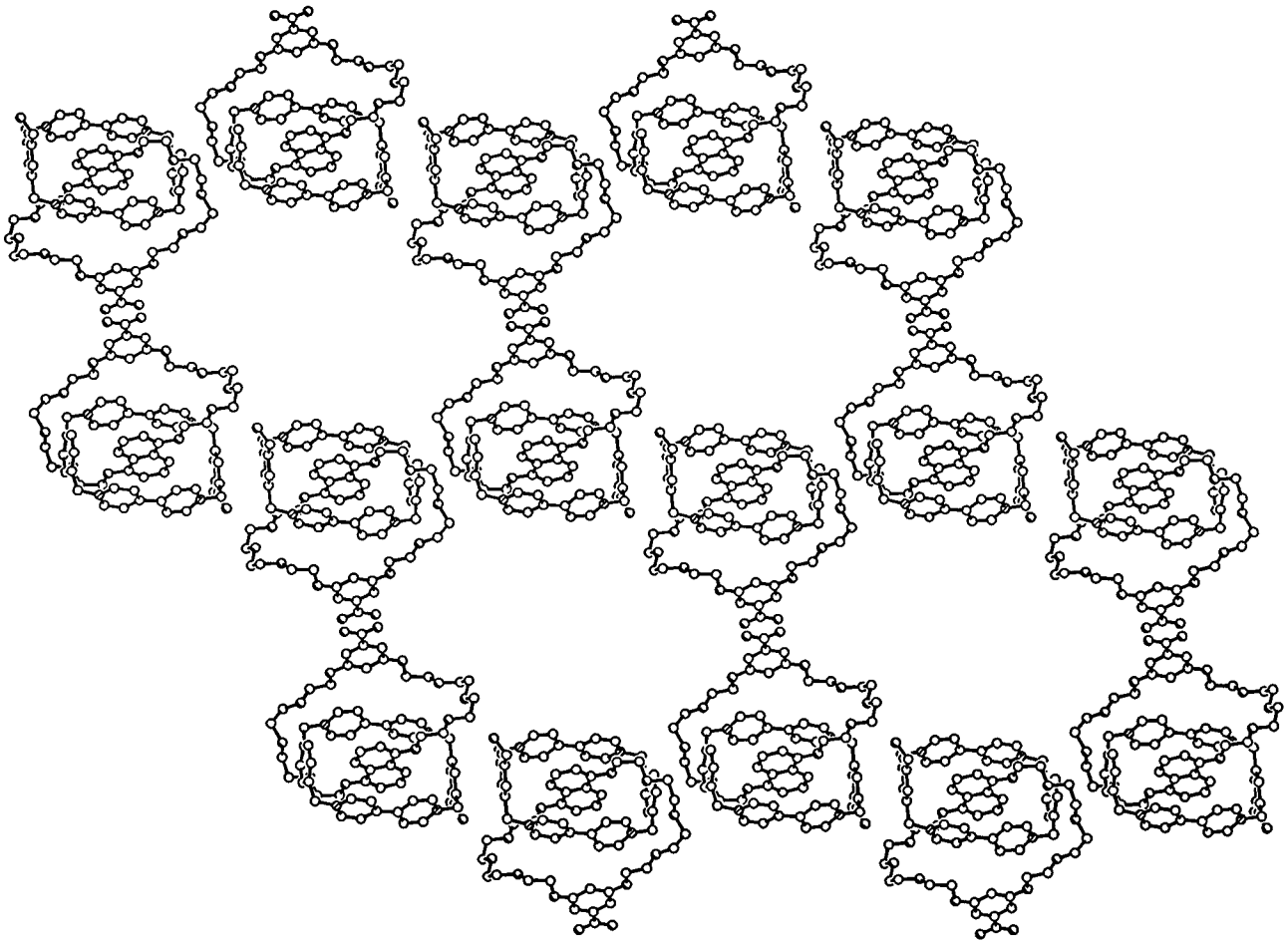

Figure 9. One of the layers formed by the [2]catenane **17**·4PF_6 in the crystal as a result of intermolecular hydrogen bonding interactions between the carboxylic acid functions and $\pi-\pi$ stacking between the centrosymmetrically related phenylene spacers adjacent molecules.

inside the cavity of the tetracationic cyclophane component of **9**·4PF_6 and **10**·4PF_6 can be distinguished. The ^{1}H-NMR spectra, recorded in CD_3CN at room temperature, show (Table 3) singlets centered on δ 6.17 and 6.21 for **9**·4PF_6 and **10**·4PF_6, respectively, corresponding to the *alongside* hydroquinone ring protons. On the contrary, as a result of the shielding effect exerted by the sandwiching bipyridinium units, the protons attached to the *inside* hydroquinone rings resonate at δ 3.29 for both **9**·4PF_6 and **10**·4PF_6. When CD_3CN solutions of the [2]catenanes **9**·4PF_6 and **10**·4PF_6 are heated, process I becomes faster on the ^{1}H-NMR time scale and broadening of the signals associated with *alongside* and *inside* hydroquinone rings is observed in the ^{1}H-NMR spectra. Coalescence of these resonances occurs at *ca.* 350 K, affording only one signal for the now indistinguishable hydroquinone rings. When the approximate line broadening treatment is employed,[19] a free energy barrier of 16.3 kcal mol^{-1} for process I was determined (Table 4) for both the [2]catenanes **9**·4PF_6 and **10**·4PF_6 at 334 K. The appearance of only two sets of signals for the hydrogen atoms H_α, attached to the α-positions with respect to the nitrogen atoms on the bipyridinium units, in the ^{1}H-NMR spectra of **9**·4PF_6 and **10**·4PF_6, recorded in CD_3CN (Table 3 and Figure 12a) at room temperature, indicates that process II is fast on the ^{1}H-NMR time scale at this temperature—*i.e.*, the *alongside* and *inside* bipyridinium units are undergoing fast exchange. When the solutions are allowed to cool down, the rate of process II decreases and the ^{1}H-NMR spectra in CD_3CN at 238 K reveal (Figure 12c) three sets of signals, integrating in a ratio of 1:1:2 for both [2]catenanes. Coalescence of the two resonances of equal intensities is observed (Figure 12b) at 250 K. When the approximate coalescence treatment is employed, a free energy barrier of 12.0 kcal mol^{-1} for process II was determined (Table 4) for both the [2]catenanes **9**·4PF_6 and **10**·4PF_6 at 238 K.

In the case of the monofunctionalized [2]catenanes **13**·4PF_6 and **14**·4PF_6 and of the difunctionalized [2]-catenanes **15**·4PF_6, **16**·4PF_6, **17**·4PF_6, and **18**·4PF_6, the 1,5-dioxynaphthalene unit incorporated within the macrocyclic polyether component is located[20] preferentially *inside* the cavity of the tetracationic cyclophane component. As a result, the hydrogen atoms attached to the 4- and 8-positions of the 1,5-dioxynaphthalene unit are shifted significantly upfield, as observed (Table 3) in the ^{1}H-NMR spectra recorded in CD_3CN at room temperature. Furthermore, the local C_2 symmetry induced by the 1,5-dioxynaphthalene unit on the tetracationic component is revealed by the appearance (Table 3), in the ^{1}H-NMR spectra, of two and four sets of signals for the hydrogen atoms H_α for the monofunctionalized [2]catenanes **13**·4PF_6 and **14**·4PF_6 and for the difunctionalized [2]catenanes **15**·4PF_6, **16**·4PF_6, **17**·4PF_6, and **18**·4PF_6 (Figure 13c), respectively. On cooling down CD_3COCD_3 solutions of these [2]catenanes, the circumrotation of the tetracationic cyclophane through the cavity of the macrocyclic polyether becomes slow on the ^{1}H-NMR time scale—*i.e.*, the *alongside* and *inside* bipyridinium units can be distinguished. As a result, the two and four sets of signals observed for H_α

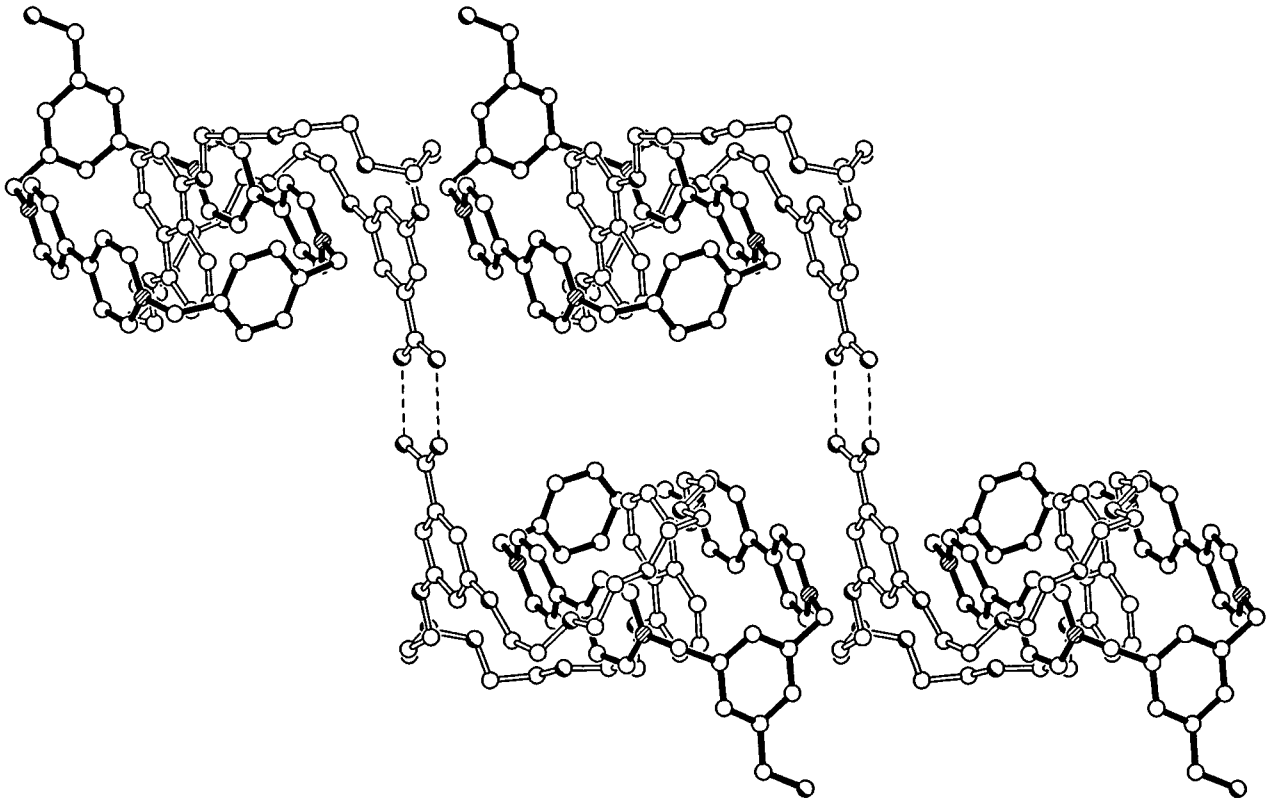

Figure 10. Intermolecular hydrogen bonding interactions between the carboxylic acid functions of adjacent [2]catenanes and continuous donor-acceptor stacks formed by **17**·4PF_6 in the crystal.

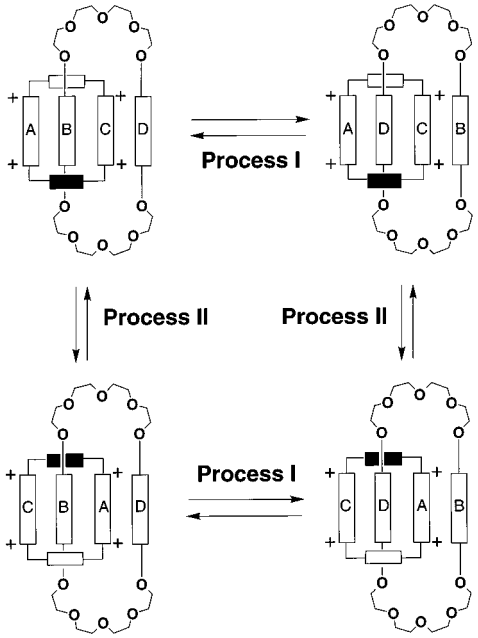

Figure 11. Schematic representation of the dynamic processes associated with the [2]catenanes **9**·4PF_6 and **10**·4PF_6 in solution.

separate into four and eight sets of resonances, respectively, for the monofunctionalized [2]catenanes **13**·4PF_6 and **14**·4PF_6 and for the difunctionalized [2]catenanes **15**·4PF_6, **16**·4PF_6, **17**·4PF_6, and **18**·4PF_6 (Figure 13e), respectively. When the approximate coalescence treatment is employed, the free energy barriers for process II listed in Table 3 were determined. When CD_3CN solutions of the monofunctionalized [2]catenanes **13**·4PF_6 and **14**·4PF_6 and the difunctionalized (Figure 13a,b) [2]catenanes **15**·4PF_6, **16**·4PF_6, **17**·4PF_6, and **18**·4PF_6 are heated up, the two and four sets of signals observed in the ^{1}H-NMR recorded at room temperature coalesce to one and two isochronous resonances, respectively. The degenerate site exchange processes responsible for the coalescence of the H_α resonances are illustrated in Figure 14. Process IIIa involves (i) dislodgement of the 1,5-dioxynaphthalene unit from the cavity of the tetracationic cyclophane, (ii) 180° rotation of the 1,5-dioxynaphthalene unit, and (iii) reinsertion of the 1,5-dioxynaphthalene unit into the cavity of the tetracationic cyclophane. Alternatively, Process IIIb involves (i) dislodgement of the 1,5-dioxynaphthalene unit from the cavity of the tetracationic cyclophane, (ii) a 180° rotation of the bipyridinium units with respect to their N···N axes, and (iii) reinsertion of the 1,5-dioxynaphthalene unit into the cavity of the tetracationic cyclophane. However, processes IIIa and IIIb cannot be distinguished by variable-temperature ^{1}H-NMR spectroscopy and the free energy barrier associated with whichever of these two dynamic processes was measured (Table 4) by employing the approximate coalescence treatment.

Polymerizations. In order to assess the versatility of the proposed (Figure 1) synthetic approaches to polycatenanes, the polyesterifications of the [2]catenanes **16**·4PF_6 and **17**·4PF_6, incorporating one hydroxymethyl group within one of their two macrocyclic components and one carboxylic acid function on the other, were attempted in various solvents and under several different conditions following literature procedures.[21] However, no oligo- and/or poly-catenanes were obtained in any case. Similarly, copolymerizations of the diacid [2]catenane **15**·4PF_6 and hydroquinone, as well as of the bis(hydroxymethyl) [2]catenane **18**·4PF_6 and terephthalic acid were attempted under the same conditions. Again, no oligo- and/or polycatenanes were

Table 3. ^{1}H-NMR Spectroscopic Data (δ Values) for [2]Catenanes 9·4PF$_6$, 10·4PF$_6$, 13·4PF$_6$, 14·4PF$_6$, 15·4PF$_6$, 16·4PF$_6$, 17·4PF$_6$, and 18·4PF$_6$ and for the Macrocyclic Polyethers 4, 6, and 12 in CD$_3$CN at Room Temperature

			neutral component				
	polycationic component		1,5-dioxynaphthalene[c]			hydroquinone[d]	
compound	H_α[a]	H_β[b]	H-2/6	H-3/7	H-4/8	alongside	inside
4			7.80−7.84	7.40−7.43	7.15−18		
6						6.73	
9·4PF$_6$	8.82, 8.71	7.69, 7.64				6.17	3.29
10·4PF$_6$	8.96, 8.74	7.66−7.76				6.21	3.29
12			7.79−7.83	7.39−7.43	7.15−7.18		
13·4PF$_6$	9.02, 8.52	7.10[e]	6.20−6.23	5.92−5.95	2.40−2.43		
14·4PF$_6$	9.02, 8.52	7.10[e]	6.20−6.23	5.92−5.95	2.40−2.43		
15·4PF$_6$	9.08, 8.85, 8.75, 8.30	6.89−7.25	6.29−6.32	5.64−6.08	2.37−2.40		
16·4PF$_6$	9.02, 8.80, 8.72, 8.40	7.01−7.18	6.29−6.32	5.64−6.24	2.27−2.30		
17·4PF$_6$	9.08, 8.85, 8.50, 8.25	7.09−7.20	6.25−6.28	5.65−6.10	2.40−2.43		
18·4PF$_6$	9.08, 8.90, 8.55, 8.40	7.03−7.17	5.61−6.13	5.61−6.13	2.40−2.43		

[a] Hydrogen atoms in the α-positions with respect to the nitrogen atoms on the bipyridinium units. [b] Hydrogen atoms in the β-positions with respect to the nitrogen atoms on the bipyridinium units. [c] Hydrogen atoms attached to the 1,5-dioxynaphthalene unit incorporated within the macrocyclic polyether component. [d] Hydrogen atoms attached to the hydroquinone rings residing alongside and inside the cavity of tetracationic cyclophane component. [e] Despite the local asymmetry imposed by the 1,5-dioxynaphthalene unit on the tetracationic cyclophane, the hydrogen atoms in the β-positions with respect to the nitrogen atoms on the bipyridnium units give rise to only one doublet centered on the δ value listed.

Table 4. Free Energy Barriers for the Dynamic Processes[a] Associated with the [2]Catenanes 9·4PF$_6$, 10·4PF$_6$, 13·4PF$_6$, 15·4PF$_6$, 16·4PF$_6$, 17·4PF$_6$, and 18·4PF$_6$ in Solution

	process I		process II		process III	
compound	$\Delta G^{\ddagger}$[b] (kcal mol^{-1})	T[b] (K)	$\Delta G_c^{\ddagger}$[c] (kcal mol^{-1})	T_c[c] (K)	$\Delta G_c^{\ddagger}$[c] (kcal mol^{-1})	T_c[c] (K)
9·4PF$_6$	16.3	334	12.0	243		
10·4PF$_6$	16.3	334	12.0	243		
13·4PF$_6$			11.1	240	16.3	347
14·4PF$_6$			11.1	240	16.3	347
15·4PF$_6$			12.0	263	16.3	347
16·4PF$_6$			12.0	263	16.3	347
17·4PF$_6$			12.0	263	16.3	347
18·4PF$_6$			12.0	263	16.4	347

[a] The dynamic processes I, II, and III are illustrated schematically in Figures 11 and 14. [b] The free energy barrier $\Delta G^{\ddagger}$ (error ± 0.2 kcal mol^{-1}) was detemined at temperature T by variable-temperature ^{1}H-NMR (400 MHz) in CD$_3$CN by empolying the approximate line broadening treatment (Sandström, J. *Dynamic NMR Spectroscopy*; Academic Press: London, 1982). The hydroquinone protons were employed as the probe. [c] The free energy barrier $\Delta G_c^{\ddagger}$ (error ± 0.2 kcal mol^{-1}) was detemined at the coalescence temperature T_c by variable temperature ^{1}H-NMR (400 MHz) in CD$_3$CN for **9**·4PF$_6$ and **10**·4PF$_6$ and in CD$_3$COCD$_3$ for **13**·4PF$_6$, **14**·4PF$_6$, **15**·4PF$_6$, **16**·4PF$_6$, **17**·4PF$_6$, and **18**·4PF$_6$ by empolying the approximate coalescence treatment (Sandström, J. *Dynamic NMR Spectroscopy*, Academic Press: London, 1982). The hydrogen atoms in the α-positions with respect to the nitrogen atoms on the bipyridinium units were employed as the probe.

isolated from any of the reaction mixtures. On the contrary, a main-chain oligo[2]catenane—such as the one schematically represented in Figure 1c—was synthesized starting from the difunctionalized [2]catenane **18**·4PF$_6$ bearing one hydroxymethyl group on each of its two macrocyclic components. Reaction (Scheme 4) of **18**·4PF$_6$ with equimolar amounts of bis(4-isocyanatophenyl)methane in MeCN at reflux over 2 days was followed by the addition of *t*-Bu$_4$NCl. The resulting purple precipitate was filtered off from the reaction mixture and dissolved in H$_2$O, after washing with Me$_2$CO. Addition of KPF$_6$ to the purple H$_2$O solution afforded the main-chain oligo[2]catenane **19**·4*n*PF$_6$, as a purple solid. However, as a result of the unsymmetrical nature of the difunctionalized [2]catenane **18**·4PF$_6$, the oligo[2]catenane **19**·4*n*PF$_6$ can incorporate three different "bridging motifs" along its main chain. Indeed, the diphenylmethane bridging unit can connect

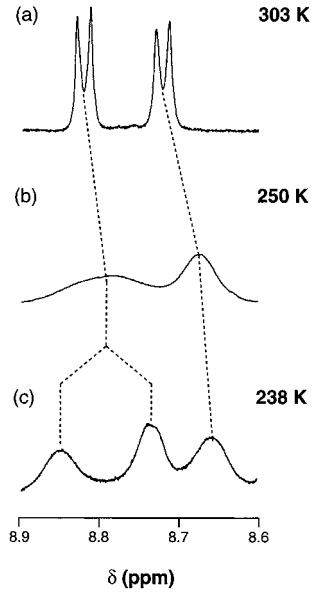

Figure 12. Partial ^{1}H-NMR spectra of the [2]catenane **10**·4PF$_6$ in CD$_3$CN at (a) 303, (b) 250, and (c) 238 K.

(a) two identical π-electron-rich or (b) two identical π-electron-deficient macrocyclic components of two adjacent [2]catenane repeating units along the oligomer backbone or (c) it can link a π-electron-rich to a π-electron-deficient macrocyclic component. Thus, the oligo[2]catenane **19**·4*n*PF$_6$ is, presumably, a mixture of a wide range of different constitutional isomeric types. Inspection of the ^{1}H- and ^{13}C-NMR spectra of **19**·4*n*PF$_6$ revealed resonances characteristic of the catenated as well as of the isocyanate-derived linkers. In particular, the resonances centered on δ 4.90 and 4.40, associated with the methylene protons of the two hydroxymethyl groups of the starting difunctionalized [2]catenane **18**·4PF$_6$, are no longer present in the ^{1}H-NMR spectrum of **19**·4*n*PF$_6$. On the contrary, two resonances centered on δ 5.20 and 5.00 are observed in the case of **19**·4*n*PF$_6$ for the methylene groups showing that, indeed, condensation has occurred. In addition, the infrared spectrum of **19**·4*n*PF$_6$ shows bands at 3375 and 1734 cm^{-1} characteristic of the NH and CO groups, respectively, of urethane linkages: these bands are not observed in the case of the starting difunctionalized [2]catenane **18**·

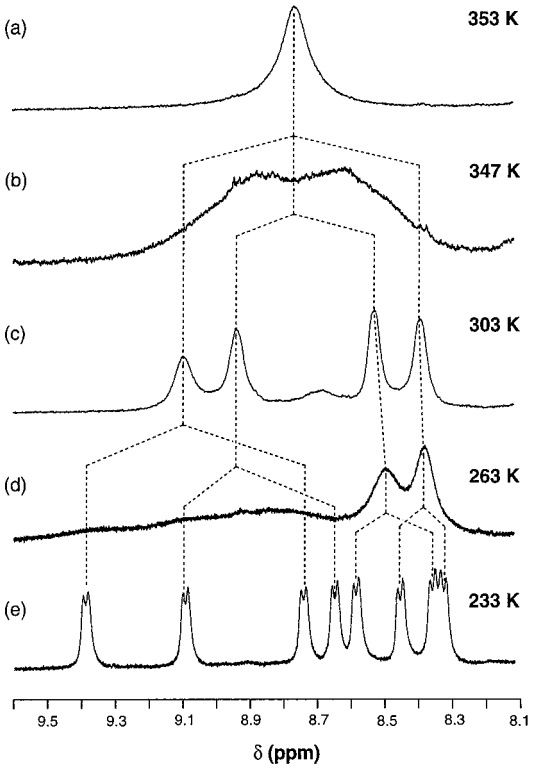

Figure 13. Partial ^{1}H-NMR spectra of the [2]catenane **18**·4PF$_6$ in CD_3CN at (a) 353 and (b) 347 K as well as in CD_3-$COCD_3$ at (c) 303, (d) 263, and (e) 233 K.

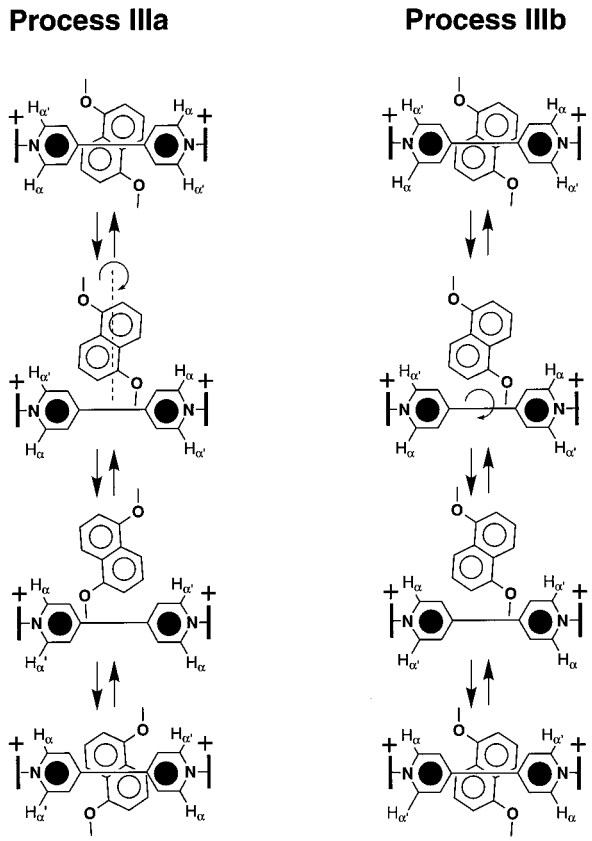

Figure 14. Dynamic processes associated with the monofunctionalized [2]catenanes **13**·4PF$_6$ and **14**·4PF$_6$ and the difunctionalized [2]catenanes **15**·4PF$_6$, **16**·4PF$_6$, **17**·4PF$_6$, and **18**·4PF$_6$ in solution.

4PF$_6$. Furthermore, the bands characteristic of allophanate linkages—*i.e.*, common side-products of condensations of isocyanates—are not observed in the infrared spectrum of **19**·4*n*PF$_6$. A number-average molecular weight M_n of 26.5 kg mol^{-1} was determined by gel permeation chromatography (GPC) performed on the chloride salt of the oligo[2]catenane **19**·4*n*Cl. A degree of polymerization of 17 based on M_n was calculated—*i.e.*, the main-chain oligo[2]catenane **19**·4*n*Cl incorporates 17 [2]catenane repeating units. The choice of proteins as standards for the determination of M_n by GPC has to be considered with some care since the radii of gyration greatly differ between globular and linear structures and hence a correlation between the two is far from satisfactory: it is the best we can do under the circumstances.

Scheme 4

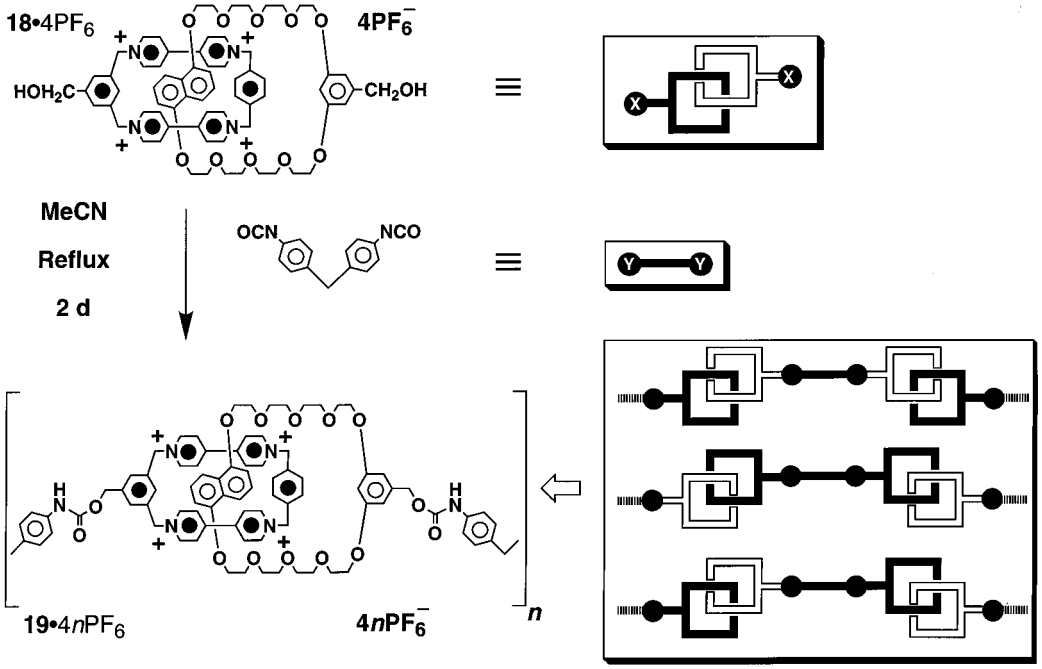

Conclusions

We have self-assembled a series of mono- and difunctionalized [2]catenanes incorporating π-electron deficient bipyridinium-based cyclophane components interlocked with dioxyarene-based macrocyclic polyether components. Reactive functional groups, such as hydroxymethyl groups and/or carboxylic acid functions, have been introduced into such monomers. In principle, condensations at these reactive groups can be employed as the polymerization or copolymerization steps. Unfortunately, presumably as a result of unfavorable stereoelectronic effects which decrease the reactivity of the functional groups directly attached to the [2]catenane monomers, the polyesterifications and copolyesterifications attempted did not afford any oligomeric or polymeric products. However, this design logic has been used successfully to synthesize a main-chain oligo[2]catenane incorporating 17 [2]catenane repeating units by reacting a monomeric difunctionalized [2]catenane bearing one hydroxymethyl group on each of its two macrocyclic components with a diisocyanate, thus affording urethane linkages.

Acknowledgment. This research was supported in the United Kingdom by the Engineering and Physical Sciences Research Council, the European Community Human Capital and Mobility Programme, and the North Atlantic Treaty Organization (Collaborative Research Grant No. 960659).

Supporting Information Available: Tables listing atomic coordinates, temperature factors, bond lengths and angles, and torsion angles and structural and crystallographic drawings of **10**·4PF_6, **13**·4PF_6, **14**·4PF_6, and **17**·4PF_6 and a table of structure factors for **10**·4PF_6 (60 pages). See any current masthead page for ordering information and Internet access instructions.

References and Notes

(1) (a) Mark, J. E. *New J. Chem.* **1993**, *17*, 703−709. (b) Lipatov, Y.; Nizel'sky, Y. *New J. Chem.* **1993**, *17*, 715−722. (c) Wood, B. R.; Semlyen, J. A. *Polymer* **1994**, *35*, 1542−1548. (d) Gibson, H. W.; Bheda, M. C.; Engen, P. T. *Prog. Polym. Sci.* **1994**, *19*, 843−945. (e) Ashton, P. R.; Preece, J. A.; Stoddart, J. F.; Tolley, M. S. *Synlett* **1994**, 789−792. (f) Preece, J. A.; Stoddart, J. F. *Macromol. Symp.* **1995**, *98*, 527−540. (g) Geerts, Y.; Muscat, D.; Müllen, K. *Macromol. Chem. Phys.* **1995**, *196*, 3425−3435. (h) Weidmann, J. L.; Kern, J. M.; Sauvage, J.-P., Geerts, Y.; Muscat, D.; Müllen, K. *J. Chem. Soc., Chem. Commun.* **1996**, 1243−1244. (i) Muscat, D.; Witte, A.; Kohler, W.; Müllen, K.; Geerts, Y. *Macromol. Commun.* **1997**, *18*, 233−241.

(2) Amabilino, D. B.; Ashton, P. R.; Reder, A. S.; Spencer, N.; Stoddart, J. F. *Angew. Chem., Int. Ed. Engl.* **1994**, *33*, 1286−1290. For the five-stage self-assembly of a branched [7]catenane, see: Amabilino, D. B.; Ashton, P. R.; Boyd, S. E.; Lee, J. Y.; Menzer, S.; Stoddart, J. F.; Williams, D. J. *Angew. Chem., Int. Ed. Engl.* **1997**, *36*, 2070−2072.

(3) (a) Schill, G. *Catenanes, Rotaxanes and Knots*, Academic Press: New York, 1971. (b) Walba, D. M. *Tetrahedron* **1985**, *41*, 3161−3212. (c) Chambron, J.-C.; Dietrich-Buchecker, C. O.; Sauvage, J.-P. *Top. Curr. Chem.* **1993**, *165*, 131−162. (c) Amabilino, D. B.; Stoddart, J. F. *Chem. Rev.* **1995**, *95*, 2725−2828. (d) Belohradsky, M.; Raymo, F. M.; Stoddart, J. F. *Collect. Czech. Chem. Commun.* **1996**, *61*, 1−43 and **1997**, *62*, 527−557.

(4) Amabilino, D. B.; Raymo, F. M.; Stoddart, J. F. In *Comprehensive Supramolecular Chemistry*; Hosseini, M. W., Sauvage J.-P., Eds.; Pergamon Press: Cambridge, England, 1996; Vol. 9, 85−130.

(5) (a) Lindsey, J. S. *New J. Chem.* **1991**, *15*, 153−180. (b) Whitesides, G. M.; Mathias, J. P.; Seto, C. T. *Science* **1991**, *254*, 1312−1319. (c) Menger, F. M.; Lee, S. S.; Tao, X. *Adv. Mater.* **1995**, *7*, 669−671. (d) Ghadiri, M. R. *Adv. Mater.* **1995**, *7*, 675−677. (e) Hunter, C. A. *Angew. Chem., Int. Ed. Engl.* **1995**, *34*, 1079−1081. (f) Lawrence, D. S.; Jiang, T.; Levett, M. *Chem. Rev.* **1995**, *95*, 2229−2260. (g) Raymo, F. M.; Stoddart, J. F. *Curr. Opin. Colloid Interface Sci.* **1996**, *1*, 116−126.

(6) (a) Schneider, H.-J. *Angew. Chem., Int. Ed. Engl.* **1991**, *30*, 1417−1436. (b) Williams, J. H. *Acc. Chem. Res.* **1993**, *26*, 593−598. (c) Hunter, C. A. *Angew. Chem., Int. Ed. Engl.* **1993**, *32*, 1584−1586. (d) Dahl, T. *Acta Chem. Scand.* **1994**, *48*, 95−116. (e) Cozzi, F.; Siegel, J. S. *Pure Appl. Chem.* **1995**, *67*, 683−689. (f) Shetty, A. S.; Zhang, J.; Moore, J. S. *J. Am. Chem. Soc.* **1996**, *118*, 1019−1027.

(7) For examples of catenanes self-assembled as a result of $\pi-\pi$ stacking and edge-to-face interactions and [C−H···O] hydrogen bonding, see: (a) Anelli, P. L.; Ashton, P. R.; Ballardini, R.; Balzani, V.; Delgado, M.; Gandolfi, M. T.; Goodnow, T. T.; Kaifer, A. E.; Philp, D.; Pietraszkiewicz, M.; Prodi, L.; Reddington, M. V.; Slawin, A. M. Z.; Spencer, N.; Stoddart, J. F.; Vicent, C.; Williams, D. J. *J. Am. Chem. Soc.* **1992**, *114*, 193−218. (b) Ashton, P. R.; Huff, J.; Menzer, S.; Parsons, I. W.; Preece, J. A.; Stoddart, J. F.; Tolley, M. S.; White, A. J. P.; Williams, D J. *Chem. Eur. J.* **1996**, *2*, 31−44.

(8) (a) Zaworotko, M. J. *Chem. Soc. Rev.* **1994**, *23*, 283−288. (b) Nishio, M.; Umezawa, Y.; Hirota, M.; Takeuchi, Y. *Tetrahedron* **1995**, *51*, 8665−8701.

(9) (a) Etter, M. *Acc. Chem. Res.* **1990**, *23*, 120−126. (b) Rebek, J., Jr. *Angew. Chem., Int. Ed. Engl.* **1990**, *29*, 245−255. (c) Desiraju, G. R. *Acc. Chem. Res.* **1991**, *24*, 290−296. (d) Aakeröy, C. B.; Seddon, K. R. *Chem. Soc. Rev.* **1993**, *22*, 397−407. (e) Lehn, J. M. *Pure Appl. Chem.* **1994**, *66*, 1961−1966. (f) Platts, J. A.; Howard, S. T.; Bracke, B. R. F. *J. Am. Chem. Soc.* **1996**, *118*, 2726−2733.

(10) For examples of catenanes self-assembled as a result of hydrogen-bonding interactions, see: (a) Hunter, C. A. *J. Am. Chem. Soc.* **1992**, *114*, 5303−5311. (b) Vögtle, F.; Meier, S.; Hoss, R. *Angew. Chem., Int. Ed. Engl.* **1992**, *31*, 1619−1622. (c) Leigh, D. A.; Moody, K.; Smart, J. P.; Watson, K. J.; Slawin, A. M.Z. *Angew. Chem., Int. Ed. Engl.* **1996**, *35*, 306−310.

(11) Furniss, B. S.; Hannaford, A. J.; Smith, P. W. G.; Tatchell, A. R. *Practical Organic Chemistry*; Longman: New York, 1989.

(12) Delaviz, Y.; Gibson, H. W. *Macromolecules* **1992**, *25*, 18−20.

(13) Engel, M.; Burris, C. W.; Slate, C. A.; Erickson, B. W. *Tetrahedron* **1993**, *49*, 8761−8770.

(14) Ashton, P. R.; Parsons, I. W.; Tolley, M. S.; Stoddart, J. F. *Chem. Eur. J.*, in preparation.

(15) Pharmacia Biotech *Gel Filtration Principles and Methods*; Rahms i Lund: Lund, Sweden, 1993.

(16) SHELXTL PC version 5.03, Siemens Analytical X-ray Instruments, Inc., Madison, WI, 1994.

(17) McRee, D. E. XtalView 3.1. Computational Center for Macromolecular Structures, San Diego Supercomputer Center, San Diego, CA, 1996.

(18) Isaacs, N. S. *Tetrahedron* **1991**, *47*, 8463−8497.

(19) (a) Sutherland, I. O. *Annu. Rep. NMR Spectrosc.* **1971**, *4*, 71−235. (b) Sandström, J. *Dynamic NMR Spectroscopy*; Academic Press: London, 1982.

(20) In the ^{1}H-NMR spectra, signals associated with the protons attached to the dioxybenzene units incorporated within the macrocyclic polyether components of the [2]catenanes **13**·4PF_6, **14**·4PF_6, **15**·4PF_6, **16**·4PF_6, **17**·4PF_6, and **18**·4PF_6 are not shifted significantly with respect to the signals for the corresponding protons in the *free* macrocyclic polyethers **4** or **12**. Furthermore, these protons resonate at approximately the same δ values and with the same intensities over the range of temperatures investigated. These observations suggest that the dioxybenzene unit does not reside inside the cavity of the tetracationic cyclophane in any of the [2]catenanes.

(21) (a) Diago-Meseguer, J.; Palomo-Coll, A. L.; Fernández-Lizabre, J. R.; Zugaza-Bilbao, A. *Synthesis* **1980**, 547−551. (b) Ueda, M.; Oikawa, H. *J. Org. Chem.* **1985**, *50*, 760−763. (c) Moore, J. S.; Stupp, S. I. *Macromolecules* **1990**, *23*, 65−70.

MA970685W